Monatsh Chem
DOI 10.1007/s00706-013-1052-1

ORIGINAL PAPER

Solvatochromic and quantum chemical investigations of newly synthesized succinimides: substituent effect on intramolecular charge transfer

Nebojša Banjac · Nemanja Trišović · Željko Vitnik · Vesna Vitnik · Nataša Valentić · Gordana Uščumlić · Ivan Juranić

Received: 14 February 2013 / Accepted: 5 July 2013

Abstract Two series of 1-aryl-3-phenyl- and 1-aryl-3,3-diphenylpyrrolidine-2,5-diones were synthesized and their solvatochromic properties were studied in a set of 15 solvents of different polarity. The effect of specific and non-specific solvent–solute interactions on the position of their absorption bands was evaluated by using the solvent parameter sets of Kamlet and Taft. The interpretation of the effect of different substituent patterns on the solvatochromic properties of the investigated compounds was based on quantum chemical calculations performed by the density functional theory (DFT)/CAM-B3LYP method using the 6-311G(d,p) basis set. The theoretical absorption frequencies show very good agreement with the experimental values. The energy gaps between the HOMO and LUMO orbitals were also analyzed. It is demonstrated that different substituents change the conjugation effect and further determine the pathways of intramolecular charge transfer.

Keywords Succinimides · Absorption spectra · Solvent effect · Quantum chemical calculations

Electronic supplementary material The online version of this article (doi:10.1007/s00706-013-1052-1) contains supplementary material, which is available to authorized users.

N. Banjac · N. Trišović · N. Valentić · G. Uščumlić (✉)
Faculty of Technology and Metallurgy,
University of Belgrade, Belgrade, Serbia
e-mail: goca@tmf.bg.ac.rs

Ž. Vitnik
Faculty of Chemistry, University of Belgrade,
Belgrade, Serbia

V. Vitnik · I. Juranić
Department of Chemistry, IChTM-Institute of Chemistry,
Technology, and Metallurgy, University of Belgrade,
Belgrade, Serbia

Introduction

Succinimides (pyrrolidine-2,5-diones) are commonly used anticonvulsant drugs in the management of absence (petit mal) seizures. They suppress the paroxysmal 3 Hz spike-and-wave activity associated with lapses of consciousness; thus, the frequency of seizures is reduced and the seizure threshold increases [1]. The therapeutic action of succinimide anticonvulsants results primarily from a decrease in T-type calcium channel activity [2, 3]. Ethosuximide (3-ethyl-3-methylpyrrolidine-2,5-dione) is the most commonly used among these anticonvulsants, whereas methsuximide (1,3-dimethyl-3-phenylpyrrolidine-2,5-dione) can be especially useful in conjunction with other anticonvulsants (e.g., phenytoin and phenobarbital) in the management of some cases of partial seizures with complex symptomatology [4]. Phensuximide (1-methyl-3-phenylpyrrolidine-2,5-dione) is the least toxic, but the least effective of the succinimide anticonvulsants and its beneficial effects often decrease during long-term therapy [4]. Because monotherapy with classical anticonvulsants sometimes fails, patients need additional drugs or a novel one to suppress seizures. Experimental evidence indicates that succinimides may be good candidates for new anticonvulsants, because many of them are effective in the maximal electroshock (MES) and subcutaneous pentylenetetrazole (scPTZ) screens that are established as standards in the early stages of drug testing [5–7].

In the search of new central nervous system (CNS)-active drug candidates, key features of a molecule which promote its interaction with a specific receptor have often been identified through the analysis of the potential of the interaction of that molecule with other systems in its vicinity [8]. The computation of the molecular electrostatic potential energy (MEP) distribution has enabled the

Published online: 15 August 2013

distinction between active and inactive succinimides on the basis of the difference between minima of the electrostatic potential in the points close to the carbonyl oxygens of the succinimide moiety [9, 10]. This difference is positive for active derivatives and negative for inactive ones. Furthermore, regression analysis has shown a positive quantitative correlation between the activity of derivatives of 3-phenylpyrrolidin-2,5-dione in the MES test and the contribution of the substituent in the aromatic fragment to the total lipophilicity of the compound [11]. Moreover, it has been demonstrated that the maximum potency of drugs acting on the CNS is obtained for derivatives with an optimum lipophilicity (expressed as octanol–water partition coefficient, log *P*) close to 2 [12, 13]. Lipophilicity is directly related to the change in Gibbs energy of solvation of a molecule between octanol and water; its dipolarity/polarizability and hydrogen bond basicity, in particular, favor partitioning into water and thus decrease lipophilicity, whereas molecular size favors octanol [14, 15]. Because of this, the solvational characteristics of succinimides need to be taken into account to get at a better insight into the features responsible for the anticonvulsant activity and, thereby, to develop some general principles that might be helpful in the design of new active compounds.

The present research is directed towards the synthesis and characterization of two series of 1-aryl-3-phenyl- (**1a**–**1j**) and 1-aryl-3,3-diphenylpyrrolidine-2,5-diones (**2a**–**2n**) as potentially new anticonvulsant agents (Fig. 1). In our previous research [16], we established relationships between their chromatographic data and the selected

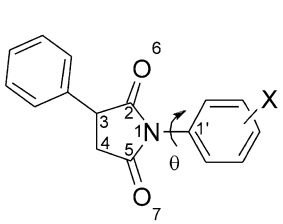

	X
1a	H
1b	4-CH_3
1c	4-OCH_3
1d	4-Cl
1e	4-Br
1f	4-NO_2
1g	4-$COCH_3$
1h	3-CH_3
1i	3-Cl
1j	3-Br

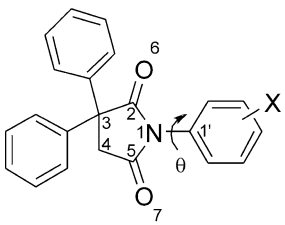

	X
2a	H
2b	4-CH_3
2c	4-OCH_3
2d	4-OH
2e	4-F
2f	4-Cl
2g	4-Br
2h	4-I
2i	4-NO_2
2j	4-CN
2k	4-$COCH_3$
2l	3-OH
2m	3-Cl
2n	3-CN

Fig. 1 Chemical structure of the investigated succinimides with the atoms and torsion angles labeled

structural features which are related to the ADMET (absorption, distribution, metabolism, excretion, and toxicity in pharmacokinetics) parameters, obtained by the established computational medicinal chemistry methods. In view of the results of this study the investigated succinimides meet the pharmacokinetic criteria of preselection of drug candidates and hence qualify for the pharmacodynamic phase of drug development. In addition, compounds **1d**, **1e**, **1i**, and **1j** appear to possess the best compromise between human intestinal absorption and plasma protein binding features. The absorption spectra of 1-aryl-3-phenyl- and 1-aryl-3,3-diphenylpyrrolidine-2,5-diones were recorded in the range from 200 to 400 nm in the selected solvents of different polarities. The effects of different substituents as well as solvent dipolarity/polarizability and solvent–solute hydrogen bonding interactions on the absorption maxima shifts were closely examined to elucidate the information relevant to the intramolecular charge transfer (ICT) within the investigated compounds. In this context, theoretical calculations were performed by the density functional theory (DFT)/CAM-B3LYP method using the 6-311G(d,p) basis set.

Results and discussion

1-Aryl-3-phenylpyrrolidine-2,5-diones **1a**–**1j** were prepared from 2-phenylsuccinic acid (**3**) and the corresponding anilines **4** under solvent-free conditions (Scheme 1). For the synthesis of 1-aryl-3,3-diphenylpyrrolidine-2,5-diones **2a**–**2n**, diphenylacetonitrile (**5**) was alkylated with ethyl bromoacetate to give the cyano-ester **6**. Hydrolysis to 2,2-diphenylsuccinic acid (**7**) and ring closure provides the anhydride **8**. The subsequent reaction of **8** with anilines **4** gives the corresponding succinimic acids **9**, which were further cyclized to 1-aryl-3,3-diphenylpyrrolidine-2,5-diones **2a**–**2n** in refluxing acetyl chloride (Scheme 2).

The absorption spectra of the investigated succinimides were recorded in the range from 200 to 400 nm in 15 solvents. The wavelengths corresponding to the most intense absorption maxima are collected in Table 1 and characteristic examples are presented in the Electronic Supplementary Material (Figs. S1–S6). Evidently, the absorption spectra show similar experimental features, i.e.,

Scheme 1

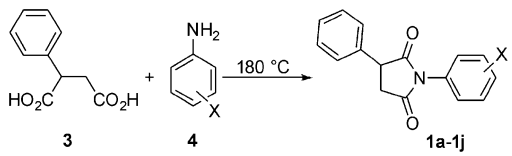

3 4 1a-1j

Scheme 2

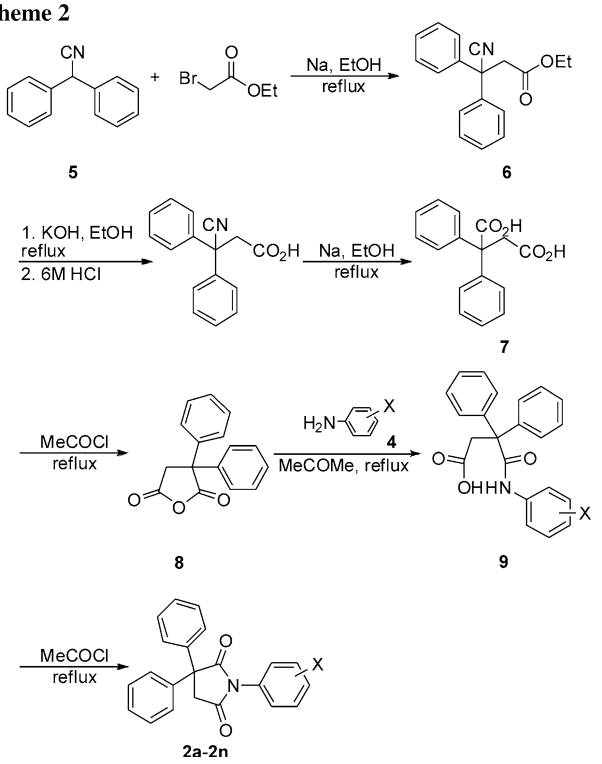

there are one or two peaks corresponding to π–π* transitions.[1] The UV absorption of the investigated succinimides is more solvent-dependent than substituent-dependent. A hypsochromic shift was observed as a function of solvent polarity and hydrogen bonding ability.

A solvatochromic study allowed us to gain an insight into the interactions of the investigated molecules with their surrounding. The effect of solvent dipolarity/polarizabilty (non-specific solvent–solute interactions) and hydrogen bonding (specific solvent–solute interactions) on the absorption maxima shifts were interpreted by using the simplified Kamlet–Taft equation [17] of the form

$$v = v_0 + s\pi^* + a\alpha \qquad (1)$$

where π^* is an index of the solvent dipolarity/polarizabilty, α is a measure of the solvent hydrogen bonding donor (HBD) acidity, and ν_0 is the regression value of this solute property in cyclohexane as reference solvent. The solvent hydrogen bond basicity parameter β is not significant in these correlations. The solvent-independent coefficients s and a in Eq. (1) measure the relative susceptibilities of the absorption maxima shift to the indicated solvent parameters.

The Kamlet–Taft parameters for the solvents used in correlations are listed in Table 2. The regression values ν_0, a, and s fit at the 95 % confidence level are given in Table 3. With exclusion of diethyl ether, diisopropyl ether, and tetrahydrofuran, correlation coefficients (R) greater than 0.98 are obtained, which indicates the high validity of the multiparameter equations and allows significant conclusions to be drawn. The degree of success of the quantification and interpretation of solvent effects on the position of the most intense absorption band is illustrated in Fig. 2 by means of a plot of ν measured (ν_{exp}) versus ν calculated (ν_{calc}) in different solvents (series 1: $R = 0.992$, sd = 0.59, $F = 7{,}922$; series 2: $R = 0.996$, sd = 0.45, $F = 16{,}197$).

The strongest influence on the solvatochromic behavior of the investigated succinimides is exerted by solvent hydrogen bond acidity. The positive sign of the coefficient a (Table 3) is caused by the hydrogen bonding between HBD solvents and the carbonyl groups, which reduces their electron density and decreases the ICT character of the chromophoric system. The investigated succinimides show positive solvatochromism with regard to the parameter π^* (as shown by the negative s coefficients in Table 3), which indicates that the electronically excited state has a higher dipole moment than the ground state and experiences stronger solvation [18, 19]. The variation in the magnitude of the s coefficient results from the different pathways of ICT which is mainly caused by electronic effects of the substituent X.

As a result of the resonant interaction with the phenyl ring, electron-donating substituents cause an increase in electron density on the oxygen atoms of the pyrrolidine-2,5-dione system (Table 4), whereby the O(6) is less electron-rich than that of O(7) owing to the vicinity of the electronegative phenyl group in position 3. This shift of electron density towards the oxygen atoms produces a polarization of the molecules and the oxygen atoms become preferred sites for the HBD attack. DFT calculations indicate non-planar conformations of the investigated succinimides (Table 5). The bond length of the carbonyl groups gets longer and the deviation from planarity (expressed in terms of dihedral angle θ, Fig. 1) decreases with increasing electron-donating ability of the substituent X. When X is an electron-accepting substituent, the polarization of the molecule results mainly from the electron-accepting competition between the aryl group in position 1 and the carbonyl groups of the succinimide moiety. The bond length of the carbonyl groups is slightly decreased and the deviation from co-planarity between these two rings is increased.

[1] Optimized structures of our compounds are of C_1 symmetry (no symmetry elements). Therefore, it is hard to identify clear π or σ orbitals, except for local molecular fragments. By visual inspection most orbitals are of π character on the benzene (phenyl) rings, but for a molecule as a whole it is impossible to define a π-nodal plane. All calculated electron transitions involve several electronic transitions among various pairs of orbitals.

Table 1 Absorption maxima of the investigated succinimides in the selected solvents

Solvent	Compound, $\nu/10^3$ cm^{-1}									
	1a	**1b**	**1c**	**1d**	**1e**	**1f**	**1g**	**1h**	**1i**	**1j**
Methanol	47.53	46.25	48.17	47.44	47.48	47.48	47.89	47.66	47.13	47.08
Ethanol	47.85	47.71	48.26	47.48	48.08	47.39	47.89	47.44	47.57	46.99
1-Propanol	47.71	47.62	48.69	47.98	48.08	47.35	47.44	47.39	47.48	46.60
2-Propanol	47.48	48.08	48.88	48.40	47.98	48.03	48.31	47.98	47.48	47.21
1-Butanol	46.86	47.89	48.03	47.04	46.99	47.17	48.08	46.73	46.73	46.43
2-Methyl-2-propanol	46.51	47.85	47.80	46.86	46.73	47.17	47.80	46.90	47.04	46.73
Diethyl ether	46.08	45.62	46.77	43.74	46.13	46.51	46.95	46.43	46.21	46.25
Diisopropyl ether	42.95	43.78	41.96	43.05	43.82	43.91	43.47	43.81	43.27	43.85
Dioxan	39.69	40.21	39.73	39.91	39.77	37.83	39.19	39.61	39.71	39.70
Tetrahydrofuran	47.52	47.91	47.72	47.17	47.73	47.87	47.43	47.52	46.79	46.37
Dimethyl sulfoxide	38.55	38.52	38.31	38.49	38.46	35.77	37.82	38.58	38.49	38.70
Methyl acetate	39.37	39.37	39.49	39.75	39.71	38.46	38.76	39.37	39.40	39.37
Ethyl acetate	39.87	39.87	39.59	39.71	39.65	36.42	38.82	39.56	39.56	39.71
N,*N*-Dimethylformamide	37.65	37.68	37.31	37.68	37.68	35.79	37.17	37.68	37.68	37.68
N,*N*-Dimethylacetamide	37.62	37.65	36.66	37.68	37.62	35.54	37.12	37.59	37.57	37.68

Solvent	Compound, $\nu/10^3$ cm^{-1}													
	2a	**2b**	**2c**	**2d**	**2e**	**2f**	**2g**	**2h**	**2i**	**2j**	**2k**	**2l**	**2m**	**2n**
Methanol	48.45	48.54	48.50	48.59	48.64	48.64	48.69	48.69	48.59	48.78	48.69	48.45	48.54	48.50
Ethanol	48.69	48.73	48.88	48.78	48.78	48.83	48.83	48.69	48.69	48.78	48.73	48.78	48.69	48.69
1-Propanol	47.89	48.03	48.08	47.98	47.85	47.89	48.08	47.94	48.03	47.89	47.98	47.94	47.98	47.85
2-Propanol	48.45	48.45	48.54	48.50	48.45	48.40	48.45	48.50	48.54	48.45	48.45	48.50	48.45	48.08
1-Butanol	48.54	48.59	48.64	48.56	48.59	48.58	48.59	48.52	48.63	48.45	48.31	48.52	48.55	48.29
2-Methylpropanol	47.94	47.98	48.02	47.86	47.96	47.94	47.88	47.79	48.01	47.62	47.33	47.85	47.92	47.15
Diethyl ether	47.21	47.21	47.44	47.30	47.08	47.13	47.26	47.35	47.35	47.35	47.35	47.35	47.44	47.13
Diisopropyl ether	43.33	43.22	43.18	42.37	43.14	42.96	42.30	42.30	43.29	41.02	39.68	42.37	43.03	41.08
Dioxan	39.59	39.59	39.37	39.59	39.59	39.59	39.59	39.22	39.43	39.22	38.91	39.59	39.59	39.59
Tetrahydrofuran	47.13	46.99	47.21	47.08	47.08	47.13	47.17	47.17	47.13	47.21	47.17	47.17	47.13	47.04
Dimethyl sulfoxide	38.37	38.34	38.28	38.28	38.31	38.37	38.37	38.20	38.26	38.14	38.11	38.31	38.37	38.28
Methyl acetate	39.40	39.46	39.59	39.49	39.43	39.53	39.53	39.49	39.40	39.56	39.43	39.56	39.56	39.59
Ethyl acetate	39.59	39.56	39.56	39.59	39.46	39.56	39.56	39.46	39.49	39.43	39.37	39.59	39.59	39.59
N,*N*-Dimethylformamide	37.57	37.57	37.54	37.57	37.57	37.57	37.54	37.51	37.48	37.37	37.37	37.37	37.57	37.57
N,*N*-Dimethylacetamide	35.56	35.56	35.61	35.49	35.56	35.56	35.56	35.59	35.41	35.49	35.49	35.36	35.64	35.54

Furthermore, we have placed emphasis on the substituent effects on the ICT process, which is relevant to the excited state properties of the investigated compounds. According to the DFT calculations, if X is an electron-donating substituent, the electron density of the HOMO orbitals is localized on the aryl group in position 1 and the imide part of the succinimide ring (**1c** and **2c**, Figs. 3 and 4). The electron density of the LUMO orbitals is mainly localized on the pyrrolidine-2,5-dione and 3-phenyl moieties. When X is a strong electron-accepting substituent, the situation is reversed (Figs. 3 and 4). The electron density of HOMO orbital for **1f** and **2i** is dominantly populated on the pyrrolidine-2,5-dione and 3-phenyl moieties, whereas the electron density of the LUMO orbitals is shifted towards the aryl group in position 1. It should be noted that the electron density of the HOMO and LUMO orbitals for **2a** is delocalized over the whole molecule which indicates their weaker ICT character than that of the other investigated succinimides.

Within the individual series of compounds, the unsubstituted compounds (**1a** and **2a**) have a larger energy gap between the HOMO and LUMO orbitals than that in the substituted ones. The energy gap of **1a** is 8.55 eV, whereas the energy gaps of **1c** and **1f** are 7.96 and 7.41 eV, respectively, and this order is consistent with the compounds of series 2. The introduction of an additional phenyl

ring into position 3 lowers the LUMO energy of the unsubstituted compound and compounds with electron-donating substituents and the HOMO energy of the compounds with an electron-accepting substituent. The net result is that the energy gap between the HOMO and LUMO orbitals is somewhat smaller for the compounds in series 2 than for corresponding compounds in series 1 with the same substituent X. It should be pointed out that the lowering of the HOMO–LUMO energy gap has a substantial influence not only on ICT, but also on the biological activity of compounds.

Finally, the MEP surface maps of compounds **1a** and **2a** indicate that the most suitable sites for electrophilic attack are O(6) and O(7) atoms, whereas the most probable sites, which can be involved in nucleophilic process, are at C(3) and C(4) atoms of the pyrrolidine-2,5-dione moiety (Fig. 5).

Table 2 Kamlet–Taft parameters of the selected solvents [17]

Solvent	π	α
Methanol	0.6	0.93
Ethanol	0.54	0.83
1-Propanol	0.52	0.78
2-Propanol	0.48	0.76
1-Butanol	0.47	0.79
2-Methyl-2-propanol	0.41	0.68
Diethyl ether	0.27	0
Diisopropyl ether	0.27	0
Dioxan	0.55	0
Tetrahydrofuran	0.58	0
Dimethyl sulfoxide	1	0
Ethyl acetate	0.55	0
Methyl acetate	0.6	0
N,*N*-Dimethylformamide	0.88	0
N,*N*-Dimethylacetamide	0.88	0

Conclusions

We have presented the synthesis and characterization of two series of 1-aryl-3-phenyl- and 1-aryl-3,3-diphenylpyrrolidine-2,5-diones. The evaluation of the solvatochromic properties of these succinimides was carried out by using the Kamlet–Taft solvent parameter scale. The strongest influence on the solvatochromic properties was exerted by specific interactions through hydrogen bonding between HBD solvents and the carbonyl groups of the succinimide moiety. With the help of quantum chemical calculations,

Table 3 Regression fits to solvent parameters

Compound	$\nu_0/10^3$ cm^{-1}	$s/10^3$ cm^{-1}	$a/10^3$ cm^{-1}	R^a	sd^b	F^c
1a	42.07 (±1.07)	−4.40 (±1.34)	9.37 (±0.63)	0.993	0.60	295
1b	43.87 (±1.66)	−6.60 (±2.08)	8.74 (±0.98)	0.985	0.92	128
1c	43.09 (±1.46)	−6.11 (±1.83)	10.37 (±0.86)	0.991	0.81	211
1d	42.76 (±1.30)	−5.19 (±1.63)	9.25 (±0.76)	0.991	0.72	208
1e	42.41 (±1.23)	−4.81 (±1.54)	9.48 (±0.72)	0.992	0.68	235
1f	41.03 (±1.50)	−5.85 (±1.88)	11.70 (±0.88)	0.992	0.83	240
1g	42.03 (±1.13)	−5.16 (±1.41)	10.59 (±0.66)	0.994	0.63	345
1h	42.01 (±1.12)	−4.37 (±1.41)	9.45 (±0.66)	0.993	0.63	271
1i	42.36 (±1.14)	−4.83 (±1.43)	9.14 (±0.67)	0.992	0.63	259
1j	42.18 (±1.04)	−4.50 (±1.31)	8.67 (±0.61)	0.993	0.58	275
2a	43.03 (±1.40)	−6.27 (±1.83)	10.59 (±0.83)	0.988	0.89	191
2b	43.04 (±1.38)	−6.29 (±1.81)	10.67 (±0.82)	0.989	0.88	198
2c	43.03 (±1.37)	−6.29 (±1.80)	10.76 (±0.81)	0.989	0.88	202
2d	43.07 (±1.39)	−6.34 (±1.82)	10.67 (±0.82)	0.989	0.89	196
2e	42.92 (±1.37)	−6.16 (±1.79)	10.73 (±0.81)	0.989	0.87	203
2f	42.99 (±1.38)	−6.19 (±1.82)	10.68 (±0.82)	0.989	0.89	196
2g	42.95 (±1.37)	−6.16 (±1.80)	10.75 (±0.81)	0.989	0.88	200
2h	42.68 (±1.31)	−5.94 (±1.72)	10.87 (±0.78)	0.990	0.84	222
2i	42.99 (±1.41)	−6.34 (±1.85)	10.81 (±0.83)	0.989	0.90	195
2j	42.66 (±1.33)	−5.98 (±1.74)	10.90 (±0.79)	0.990	0.85	218
2k	42.23 (±1.33)	−5.53 (±1.74)	11.05 (±0.79)	0.990	0.85	218
2l	43.23 (±1.46)	−6.60 (±1.92)	10.58 (±0.87)	0.987	0.94	176
2m	43.06 (±1.36)	−6.25 (±1.78)	10.59 (±0.80)	0.989	0.87	201
2n	42.76 (±1.36)	−5.92 (±1.79)	10.4 5(±0.81)	0.989	0.87	193

[a] Regression coefficient

[b] Standard deviation

[c] Fisher test

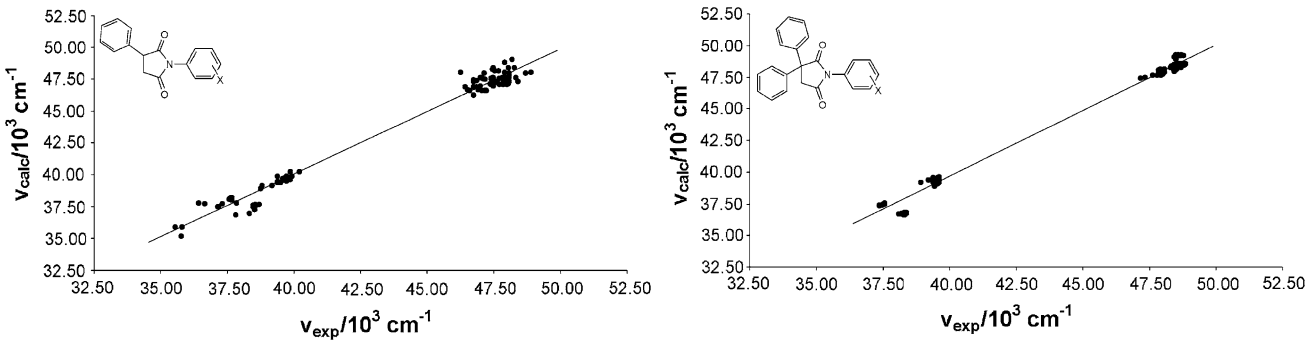

Fig. 2 Relationship between calculated and experimental values of absorption frequencies for the investigated succinimides, according to the Kamlet–Taft equation (Eq. 1)

Table 4 NBO charge of the atoms of the succinimide moiety

Compound	C(2)	N(1)	C(5)	O(6)	O(7)
1a	0.758	−0.528	0.743	−0.575	−0.579
1b	0.757	−0.527	0.743	−0.576	−0.580
1c	0.756	−0.524	0.742	−0.578	−0.581
1d	0.758	−0.528	0.744	−0.574	−0.578
1e	0.758	−0.528	0.744	−0.574	−0.578
1f	0.760	−0.533	0.746	−0.570	−0.574
1g	0.759	−0.531	0.744	−0.574	−0.575
1h	0.758	−0.528	0.743	−0.576	−0.579
1i	0.758	−0.530	0.745	−0.571	−0.577
1j	0.759	−0.530	0.744	−0.573	−0.576
2a	0.769	−0.525	0.747	−0.587	−0.576
2b	0.769	−0.523	0.747	−0.588	−0.578
2c	0.768	−0.521	0.746	−0.590	−0.578
2d	0.768	−0.521	0.746	−0.589	−0.580
2e	0.769	−0.524	0.747	−0.587	−0.577
2f	0.770	−0.525	0.748	−0.586	−0.576
2g	0.770	−0.525	0.748	−0.586	−0.576
2h	0.770	−0.525	0.748	−0.586	−0.576
2i	0.772	−0.529	0.749	−0.582	−0.573
2j	0.772	−0.529	0.749	−0.583	−0.574
2k	0.771	−0.527	0.748	−0.586	−0.573
2l	0.770	−0.526	0.747	−0.586	−0.574
2m	0.771	−0.526	0.748	−0.586	−0.574
2n	0.772	−0.528	0.749	−0.584	−0.576

the transmission of substituent effects through the molecular skeleton and the nature of the HOMO and LUMO orbitals were additionally examined. We have demonstrated that substituents on the phenyl ring in position 1 significantly change the conjugation effect and further affect the ICT character of the investigated succinimides.

This investigation of substituent effects on the solvatochromic properties controlled by the ICT character of succinimides is helpful to understand the interactions with their environment and may contribute to the design of new compounds with improved pharmacokinetic properties.

Experimental

Commercially available materials were used without further purification. The chemical structures and the purities of the synthesized succinimide derivatives were confirmed by melting points, elemental analysis, FT-IR, ^{1}H and ^{13}C NMR spectra. Elemental analysis was realized using an Elemental Vario EL III microanalyzer; the results were found to be in good agreement (±0.3 %) with the calculated values. FT-IR spectra were recorded on a Bomem MB 100 spectrometer in the form of KBr pellets. ^{1}H and ^{13}C

Table 5 Results obtained from the CAM-B3LYP/6-311G(d,p) geometry optimization (bond lengths/Å; angles/°) for the investigated succinimides

Compound	N(1)–C(2)	N(1)–C(5)	C(4)–C(5)	C(3)–C(4)	C(2)–C(3)	N(1)–C(1′)	C(2)=O(6)	C(5)=O(7)	θ
1a	1.400	1.401	1.513	1.529	1.530	1.429	1.197	1.199	42.2
1b	1.399	1.400	1.514	1.529	1.530	1.429	1.198	1.199	42.7
1c	1.398	1.399	1.514	1.529	1.530	1.429	1.198	1.199	42.8
1d	1.401	1.402	1.513	1.529	1.529	1.427	1.197	1.199	40.0
1e	1.402	1.402	1.513	1.529	1.529	1.427	1.197	1.199	39.7
1f	1.405	1.405	1.512	1.529	1.528	1.424	1.197	1.198	37.5
1g	1.402	1.404	1.513	1.529	1.529	1.426	1.197	1.198	39.4
1h	1.399	1.401	1.514	1.529	1.530	1.430	1.198	1.199	43.5
1i	1.402	1.403	1.513	1.529	1.529	1.427	1.197	1.199	40.2
1j	1.402	1.403	1.513	1.529	1.529	1.427	1.197	1.198	40.4
2a	1.397	1.401	1.509	1.537	1.541	1.429	1.199	1.199	137.7
2b	1.396	1.400	1.509	1.537	1.541	1.429	1.199	1.199	137.8
2c	1.395	1.399	1.509	1.537	1.541	1.429	1.200	1.199	136.8
2d	1.396	1.399	1.509	1.538	1.541	1.429	1.200	1.200	137.1
2e	1.397	1.401	1.509	1.537	1.540	1.428	1.199	1.199	138.5
2f	1.399	1.402	1.508	1.537	1.540	1.427	1.199	1.199	140.5
2g	1.399	1.402	1.508	1.537	1.540	1.427	1.199	1.199	140.7
2h	1.399	1.402	1.508	1.537	1.540	1.426	1.199	1.199	141.2
2i	1.403	1.405	1.507	1.537	1.538	1.423	1.198	1.198	143.1
2j	1.402	1.404	1.507	1.537	1.539	1.424	1.198	1.198	141.1
2k	1.400	1.403	1.508	1.537	1.540	1.426	1.199	1.198	140.9
2l	1.397	1.401	1.509	1.537	1.541	1.429	1.199	1.198	137.4
2m	1.399	1.402	1.508	1.537	1.540	1.426	1.199	1.198	140.0
2n	1.401	1.403	1.508	1.538	1.539	1.425	1.199	1.199	141.1
Succinimide[a]	1.361	1.380	1.513	1.524	1.504	–	1.225	1.212	

[a] Experimental values from X-ray geometry [20]

NMR spectra were recorded on a Varian Gemini 200 spectrometer at 200 MHz for the ^{1}H NMR and 50 MHz for the ^{13}C NMR spectra. The spectra were recorded at room temperature in $CDCl_3$ and DMSO-d_6. The chemical shifts are expressed in ppm relative to TMS (δ(H) = 0 ppm) in the ^{1}H NMR and the residual solvent signal ($CDCl_3$: δ(C) = 77 ppm; DMSO-d_6: δ(C) = 39.5 ppm) in the ^{13}C NMR spectra. The coupling constants J(H,H) are expressed in Hz. The UV absorption spectra were measured in spectroquality solvents (Fluka) at 1×10^{-5} mol dm^{-3} concentration with a Shimadzu 1700 spectrophotometer.

*General procedure for the preparation of 1-(3- and 4-substituted phenyl)-3-phenylpyrrolidine-2,5-diones **1a–1j***

All of the investigated 1-aryl-3-phenylpyrrolidine-2,5-diones were synthesized from 2-phenylsuccinic acid (**3**) and the corresponding aniline **4** using a modified literature procedure (Scheme 1) [21].

2-Phenylsuccinic acid (4.1 g, 0.021 mol) and the corresponding aniline (0.028 mol) were placed into 100-cm^3 flask equipped with a reflux condenser and a magnetic stirrer. The reaction mixture was heated in an oil bath at 180 °C until it became liquid. The heating was continued for a further 3 h at 180 °C. The reaction mixture was allowed to cool to room temperature, during which time it solidified. Recrystallization of the solid from an ethanol/water mixture yielded a crystalline product. The melting points, FT-IR, ^{1}H and ^{13}C NMR spectra of compounds **1a–1e** are in agreement with literature data (Table 6) and undoubtedly corroborate their structures.

1-(4-Nitrophenyl)-3-phenylpyrrolidine-2,5-dione (**1f**, $C_{16}H_{12}N_2O_4$)

Yellow crystalline solid; yield: 37 %; m.p.: 110–113 °C; IR (KBr): $\overline{\nu}$ = 1,779 (C=O), 1,711 (C=O) cm^{-1}; ^{1}H NMR (200 MHz, $CDCl_3$): δ = 8.28 (d, J = 9.6 Hz, 2H, Ar), 7.59 (d, J = 9.0 Hz, 2H, Ar), 7.45–7.25 (m, 5H, Ph), 4.22 (dd, J = 5.1 Hz, 9.5 Hz, 1H, H–C(3)), 3.40 (dd,

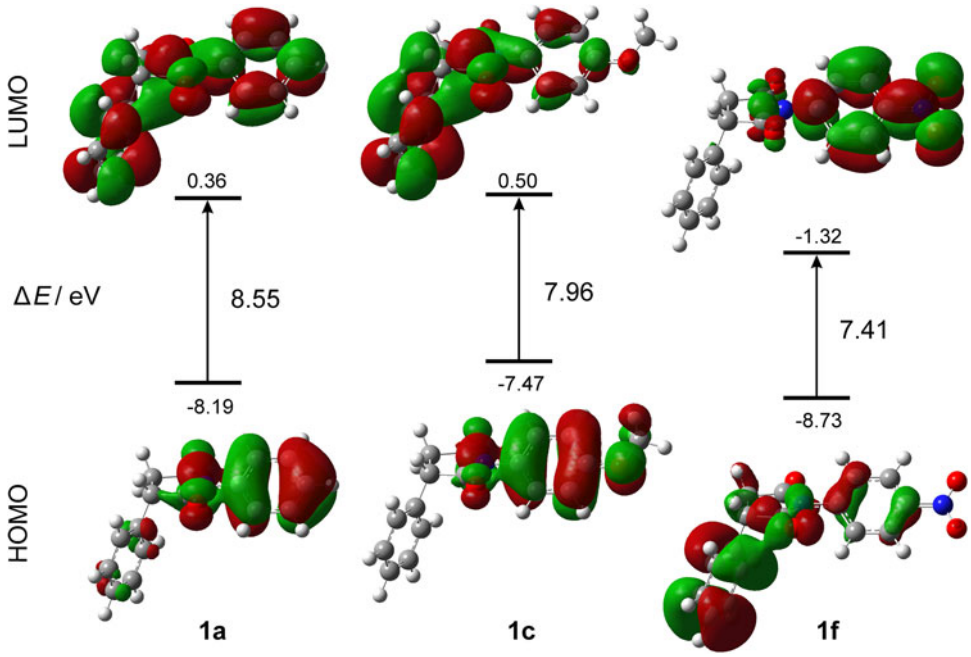

Fig. 3 Molecular orbitals and HOMO–LUMO energy gaps for **1a**, **1c**, and **1f** (color figure online)

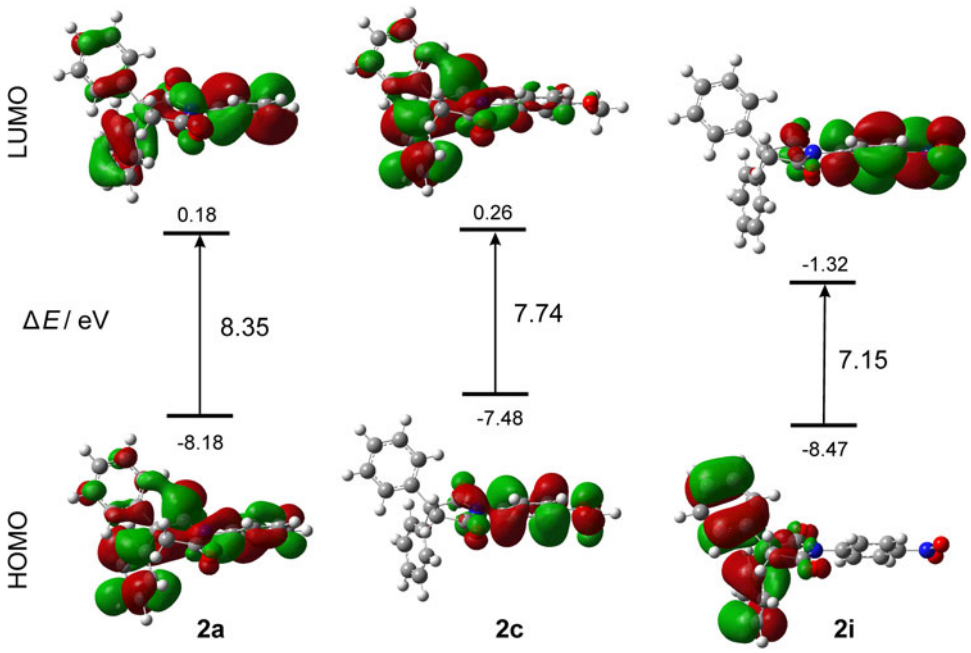

Fig. 4 Molecular orbitals and HOMO–LUMO energy gaps for **2a**, **2c**, and **2i** (color figure online)

J = 9.8 Hz, 18.8 Hz, 1H, H–C(4)), 3.02 (dd, J = 5.0 Hz, 18.6 Hz, 1H, H–C(4)) ppm; ^{13}C NMR (50 MHz, $CDCl_3$): δ = 175.9 (C(5)), 174.2 (C(2)), 146.8, 137.3, 136.4, 129.3, 128.2, 127.3, 126.8, 124.2, 45.8 (C(3)), 36.9 (C(4)) ppm.

1-(4-Acetylphenyl)-3-phenylpyrrolidine-2,5-dione (**1g**, $C_{18}H_{15}NO_3$)

White crystalline solid; yield: 29 %; m.p.: 108–113 °C; IR (KBr): $\bar{\nu}$ = 1,780 (C=O), 1,708 (C=O) cm^{-1}; ^{1}H NMR (200 MHz, $CDCl_3$): δ = 8.02 (d, J = 8.4 Hz, 2H, Ar), 7.46 (d, J = 8.4 Hz, 2H, Ph), 7.39–7.27 (m, 5H, Ar + Ph), 4.20 (dd, J = 5.0 Hz, 9.6 Hz, 1H, H–C(3)), 3.37 (dd, J = 9.8 Hz, 18.8 Hz, 1H, H–C(4)), 3.00 (dd, J = 5.1 Hz, 18.5 Hz, 1H, H–C(4)), 2.59 (s, 3H, COMe) ppm; ^{13}C NMR (50 MHz, $CDCl_3$): δ = 197.0, 176.2 (C(5)), 174.6 (C(2)), 136.7, 136.6, 135.9, 129.2, 129.0, 128.0, 127.3, 126.3, 45.8 (C(3)), 37.0 (C(4)), 26.5 ppm.

1-(3-Methylphenyl)-3-phenylpyrrolidine-2,5-dione (**1h**, $C_{17}H_{15}NO_2$)

White crystalline solid; yield: 45 %; m.p.: 84–88 °C; IR (KBr): $\bar{\nu}$ = 1,781 (C=O), 1,707 (C=O) cm^{-1}; ^{1}H NMR

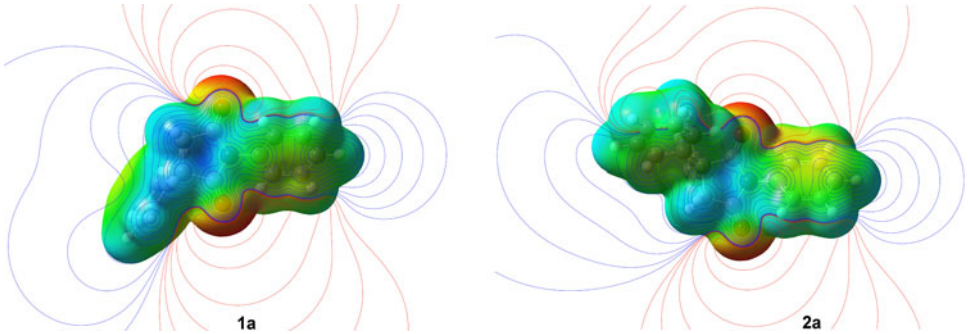

Fig. 5 Molecular electrostatic potential (MEP) maps of **1a** and **2a** (color figure online)

Table 6 Synthesis of compounds **1a**–**1e**

Compound	Yield/%	M.p./°C	
		Found	Reported
1a	53	134–137	135–138 [22]
1b	40	145–147	145–147 [22]
1c	61	162–164	161–162 [22]
1d	34	160–162	158–162 [22]
1e	34	156–158	155–158 [22]

(200 MHz, $CDCl_3$): δ = 7.42–7.07 (m, 9H, Ar + Ph), 4.12 (dd, J = 4.6 Hz, 9.6 Hz, 1H, H–C(3)), 3.30 (dd, J = 9.6 Hz, 18.4 Hz, 1H, H–C(4)), 2.92 (dd, J = 5.0 Hz, 18.6 Hz, 1H, H–C(4)), 2.36 (s, 3H, Me) ppm; ^{13}C NMR (50 MHz, $CDCl_3$): δ = 176.7 (C(5)), 175.3 (C(2)), 139.2, 137.2, 131.7, 129.5, 129.1, 128.9, 127.9, 127.3, 127.0, 123.5, 45.8 (C(3)), 37.1 (C(4)), 21.2 ppm.

1-(3-Chlorophenyl)-3-phenylpyrrolidine-2,5-dione (**1i**, $C_{16}H_{12}ClNO_2$)
White crystalline solid; yield: 39 %; m.p.: 103–107 °C; IR (KBr): $\bar{\nu}$ = 1,781 (C=O), 1,706 (C=O) cm^{-1}; ^{1}H NMR (200 MHz, $CDCl_3$): δ = 7.42–7.19 (m, 9H, Ar + Ph), 4.13 (dd, J = 5.1 Hz, 9.5 Hz, 1H, H–C(3)), 3.31 (dd, J = 9.6 Hz, 18.6 Hz, 1H, H–C(4)), 2.93 (dd, J = 5.1 Hz, 18.6 Hz, 1H, H–C(4)) ppm; ^{13}C NMR (50 MHz, $CDCl_3$): δ = 176.2 (C(5)), 174.7 (C(2)), 136.8, 134.6, 132.9, 130.0, 129.2, 128.8, 128.0, 127.3, 126.6, 124.6, 45.8 (C(3)), 36.9 (C(4)) ppm.

1-(3-Bromophenyl)-3-phenylpyrrolidine-2,5-dione (**1j**, $C_{16}H_{12}BrNO_2$)
White crystalline solid; yield: 37 %; m.p.: 99–104 °C; IR (KBr): $\bar{\nu}$ = 1,779 (C=O), 1,707 (C=O) cm^{-1}; ^{1}H NMR (200 MHz, $CDCl_3$): δ = 7.54–7.24 (m, 9H, Ar + Ph), 4.14 (dd, J = 5.0 Hz, 9.6 Hz, 1H, H–C(3)), 3.32 (dd, J = 9.6 Hz, 18.6 Hz, 1H, H–C(4)), 2.95 (dd, J = 5.0 Hz, 18.6 Hz, 1H, H–C(4)) ppm; ^{13}C NMR (50 MHz, $CDCl_3$): δ = 176.2 (C(5)), 174.6 (C(2)), 136.8, 133.0, 131.7, 130.3, 129.4, 129.2, 128.1, 127.3, 125.0, 122.3, 45.8 (C(3)), 37.0 (C(4)) ppm.

General procedure for the preparation of 1-(3- and 4-substituted phenyl)-3,3-diphenylpyrrolidine-2,5-diones ***2a–2n***

All of the investigated 1-aryl-3,3-diphenylpyrrolidine-2,5-diones were synthesized from 2,2-diphenylsuccinic acid anhydride (**8**) and the corresponding aniline **4** (Scheme 2) using a modified literature procedure [23, 24]. 2,2-Diphenylsuccinic acid anhydride (**8**) was previously synthesized by the method of Miller and Long [24].

Acetone (10 cm^3), 1.26 g 2,2-diphenylsuccinic acid anhydride (0.005 mol), and the corresponding aniline (0.005 mol) were placed into a 50-cm^3 flask equipped with a reflux condenser and a magnetic stirrer. The resulting mixture was stirred for 4 h at reflux and concentrated to remove excess acetone. The precipitated crude succinimic acid was taken in 6.5 cm^3 of acetyl chloride. The mixture was heated until the evolution of hydrogen chloride ceased. Acetyl chloride was evaporated and the crude material was filtered off and re-crystallized from acetone to yield crystalline product.

1,3,3-Triphenylpyrrolidine-2,5-dione (**2a**, $C_{22}H_{17}NO_2$)
White crystalline solid; yield: 34 %; m.p.: 158–162 °C; IR (KBr): $\bar{\nu}$ = 1,779 (C=O), 1,713 (C=O) cm^{-1}; ^{1}H NMR (200 MHz, DMSO-d_6): δ = 7.56–7.28 (m, 15H, Ph), 3.77 (s, 2H, H–C(4)) ppm; ^{13}C NMR (50 MHz, DMSO-d_6): δ = 177.7 (C(5)), 174.2 (C(2)), 142.0, 132.4, 129.3, 128.9, 127.7, 127.4, 57.1 (C(3)), 44.5 (C(4)) ppm.

1-(4-Methylphenyl)-3,3-diphenylpyrrolidine-2,5-dione (**2b**, $C_{23}H_{19}NO_2$)
White crystalline solid; yield: 31 %; m.p.: 114–116 °C; IR (KBr): $\bar{\nu}$ = 1,779 (C=O), 1,712 (C=O) cm^{-1}; ^{1}H NMR (200 MHz, DMSO-d_6): δ = 7.46–7.28 (m, 12H, Ar + Ph), 7.17 (d, J = 8.4 Hz, 2H, Ar), 3.75 (s, 2H, H–C(4)), 2.33 (s, 3H, Me) ppm; ^{13}C NMR (50 MHz, DMSO-d_6): δ = 177.8 (C(5)), 174.3 (C(2)), 142.0, 138.5, 129.8, 129.8, 128.0, 127.7, 127.1, 57.1 (C(3)), 44.4 (C(4)), 20.9 ppm.

1-(4-Methoxyphenyl)-3,3-diphenylpyrrolidine-2,5-dione (**2c**, $C_{23}H_{19}NO_3$)
Yellow crystalline solid; yield: 37 %; m.p.: 119–121 °C; IR (KBr): $\bar{\nu}$ = 1,782 (C=O), 1,717 (C=O) cm^{-1}; ^{1}H NMR

(200 MHz, DMSO-d_6): δ = 7.42–7.28 (m, 10H, Ph), 7.22 (d, J = 9 Hz, 2H, Ar), 7.05 (d, J = 9 Hz, 2H, Ar), 3.78 (s, 3H, OMe), 3.73 (s, 2H, H–C(4)) ppm; ^{13}C NMR (50 MHz, DMSO-d_6): δ = 177.9 (C(5)), 174.4 (C(2)), 159.4, 142.1, 128.9, 128.6, 127.7, 125.0, 114.5, 57.0, 55.6 (C(3)), 44.4 (C(4)) ppm.

1-(4-Hydroxyphenyl)-3,3-diphenylpyrrolidine-2,5-dione (**2d**, $C_{22}H_{17}NO_3$)
Dark crystalline solid; yield: 25 %; m.p.: 167–170 °C; IR (KBr): $\overline{\nu}$ = 1,761 (C=O), 1,711 (C=O) cm^{-1}; ^{1}H NMR (200 MHz, DMSO-d_6): δ = 9.80 (s, 1H, OH), 7.42–7.26 (m, 14H, Ar + Ph), 3.77 (s, 2H, H–C(4)) ppm; ^{13}C NMR (50 MHz, DMSO-d_6): δ = 177.7 (C(5)), 174.2 (C(2)), 150.5, 142.0, 129.9, 129.0, 128.8, 128.6, 127.8, 122.9, 57.1 (C(3)), 44.5 (C(4)) ppm.

1-(4-Fluorophenyl)-3,3-diphenylpyrrolidine-2,5-dione (**2e**, $C_{22}H_{16}FNO_2$)
White crystalline solid; yield: 27 %; m.p.: 109–111 °C; IR (KBr): $\overline{\nu}$ = 1,781 (C=O), 1,714 (C=O) cm^{-1}; ^{1}H NMR (200 MHz, DMSO-d_6): δ = 7.43–7.27 (m, 14H, Ar + Ph), 3.77 (s, 2H, H–C(4)) ppm; ^{13}C NMR (50 MHz, DMSO-d_6): δ = 177.6 (C(5)), 174.2 (C(2)), 164.3, 141.9, 129.7, 129.5, 128.9, 127.7, 116.5, 116.0, 57.1 (C(3)), 44.4 (C(4)) ppm.

1-(4-Chlorophenyl)-3,3-diphenylpyrrolidine-2,5-dione (**2f**, $C_{22}H_{16}ClNO_2$)
White crystalline solid; yield: 23 %; m.p.: 132–135 °C; IR (KBr): $\overline{\nu}$ = 1,777 (C=O), 1,711 (C=O) cm^{-1}; ^{1}H NMR (200 MHz, DMSO-d_6): δ = 7.59 (d, J = 8.8 Hz, 2H, Ar), 7.42–7.29 (m, 12H, Ar + Ph), 3.77 (s, 2H, H–C(4)) ppm; ^{13}C NMR (50 MHz, DMSO-d_6): δ = 177.5 (C(5)), 174.0 (C(2)), 141.9, 133.4, 131.2, 129.4, 129.2, 129.0, 127.7, 57.1 (C(3)), 44.4 (C(4)) ppm.

1-(4-Bromophenyl)-3,3-diphenylpyrrolidine-2,5-dione (**2g**, $C_{22}H_{16}BrNO_2$)
White crystalline solid; yield 35 %; m.p.: 150–152 °C; IR (KBr): $\overline{\nu}$ = 1,778 (C=O), 1,711 (C=O) cm^{-1}; ^{1}H NMR (200 MHz, DMSO-d_6): δ = 7.73 (d, J = 8.4 Hz, 2H, Ar), 7.42–7.28 (m, 12H, Ar + Ph), 3.77 (s, 2H, H–C(4)) ppm; ^{13}C NMR (50 MHz, DMSO-d_6): δ = 177.4 (C(5)), 174.0 (C(2)), 141.9, 132.3, 131.7, 129.5, 129.0, 127.7, 121.9, 57.1 (C(3)), 44.4 (C(4)) ppm.

1-(4-Iodophenyl)-3,3-diphenylpyrrolidine-2,5-dione (**2h**, $C_{22}H_{16}INO_2$)
White crystalline solid; yield: 25 %; m.p.: 158–160 °C; IR (KBr): $\overline{\nu}$ = 1,778 (C=O), 1,712 (C=O) cm^{-1}; ^{1}H NMR (200 MHz, DMSO-d_6): δ = 7.88 (d, J = 8.6 Hz, 2H, Ar), 7.42–7.28 (m, 10H, Ph), 7.14 (d, J = 8.4 Hz, 2H, Ar), 3.76 (s, 2H, H–C(4)) ppm; ^{13}C NMR (50 MHz, DMSO-d_6): δ = 177.4 (C(5)), 174.0 (C(2)), 141.9, 138.2, 132.1, 129.5, 129.0, 127.7, 95.0, 57.1 (C(3)), 44.4 (C(4)) ppm.

1-(4-Nitrophenyl)-3,3-diphenylpyrrolidine-2,5-dione (**2i**, $C_{22}H_{16}N_2O_4$)
White crystalline solid; yield: 29 %; m.p.: 104–106 °C; IR (KBr): $\overline{\nu}$ = 1,778 (C=O), 1,715 (C=O) cm^{-1}; ^{1}H NMR (200 MHz, DMSO-d_6): δ = 8.39 (d, J = 9 Hz, 2H, Ar), 7.68 (d, J = 9 Hz, 2H, Ar), 7.44–7.30 (m, 10H, Ph), 3.83 (s, 2H, H–C(4)) ppm; ^{13}C NMR (50 MHz, DMSO-d_6): δ = 177.2 (C(5)), 173.6 (C(2)), 147.1, 141.7, 137.9, 129.0, 128.4, 127.8, 127.7, 124.6, 57.2 (C(3)), 44.4 (C(4)) ppm.

1-(4-Cyanophenyl)-3,3-diphenylpyrrolidine-2,5-dione (**2j**, $C_{23}H_{16}N_2O_2$)
White crystalline solid; yield: 29 %; m.p.: 129–133 °C; IR (KBr): $\overline{\nu}$ = 1,782 (C=O), 1,714 (C=O) cm^{-1}; ^{1}H NMR (200 MHz, DMSO-d_6): δ = 8.01 (d, J = 8.4 Hz, 2H, Ar), 7.59 (d, J = 8.4 Hz, 2H, Ar), 7.43–7.29 (m, 10H, Ph), 3.81 (s, 2H, H–C(4)) ppm; ^{13}C NMR (50 MHz, DMSO-d_6): δ = 177.2 (C(5)), 173.7 (C(2)), 141.7, 136.4, 133.4, 129.0, 128.2, 127.8, 127.7, 118.5, 111.5, 57.2 (C(3)), 44.4 (C(4)) ppm.

1-(4-Acetylphenyl)-3,3-diphenylpyrrolidine-2,5-dione (**2k**, $C_{24}H_{19}NO_3$)
White crystalline solid; yield: 34 %; m.p.: 156–158 °C; IR (KBr): $\overline{\nu}$ = 1,781 (C=O), 1,713 (C=O) cm^{-1}; ^{1}H NMR (200 MHz, DMSO-d_6): δ = 8.09 (d, J = 8.4 Hz, 2H, Ar), 7.50 (d, J = 8.6 Hz, 2H, Ar), 7.43–7.31 (m, 10H, Ph), 3.80 (s, 2H, H–C(4)), 2.61 (s, 3H, COMe) ppm; ^{13}C NMR (50 MHz, DMSO-d_6): δ = 197.5, 177.4 (C(5)), 173.9 (C(2)), 141.8, 136.8, 136.3, 129.2, 129.0, 127.7, 127.4, 57.2 (C(3)), 44.4 (C(4)), 27.0 ppm.

1-(3-Hydroxyphenyl)-3,3-diphenylpyrrolidine-2,5-dione (**2l**, $C_{22}H_{17}NO_3$)
Dark crystalline solid; yield: 28 %; m.p.: 169–171 °C; IR (KBr): $\overline{\nu}$ = 1,778 (C=O), 1,708 (C=O) cm^{-1}; ^{1}H NMR (200 MHz, DMSO-d_6): δ = 9.81 (s, 1H, OH), 7.42–7.25 (m, 11H, Ar + Ph), 6.86 (d, J = 9.4 Hz, 1H, Ar), 6.73–6.70 (m, 2H, Ar), 3.75 (s, 2H, H–C(4)) ppm; ^{13}C NMR (50 MHz, DMSO-d_6): δ = 177.7 (C(5)), 174.2 (C(2)), 158.1, 142.0, 133.4, 130.0, 129.0, 127.8, 117.8, 115.9, 114.3, 57.1 (C(3)), 44.4 (C(4)) ppm.

1-(3-Chlorophenyl)-3,3-diphenylpyrrolidine-2,5-dione (**2m**, $C_{22}H_{16}ClNO_2$)
White crystalline solid; yield: 33 %; m.p.: 135–138 °C; IR (KBr): $\overline{\nu}$ = 1,783 (C=O), 1,713 (C=O) cm^{-1}; ^{1}H NMR (200 MHz, DMSO-d_6): δ = 7.56–7.30 (m, 14H, Ar + Ph), 3.77 (s, 2H, H–C(4)) ppm; ^{13}C NMR (50 MHz, DMSO-d_6): δ = 177.4 (C(5)), 173.9 (C(2)), 141.9, 133.7, 133.4, 131.0, 129.0, 127.8, 127.4, 126.2, 57.1 (C(3)), 44.5 (C(4)) ppm.

1-(3-Cyanophenyl)-3,3-diphenylpyrrolidine-2,5-dione (**2n**, $C_{23}H_{16}N_2O_2$)
White crystalline solid; yield: 33 %; m.p.: 129–133 °C; IR (KBr): $\overline{\nu}$ = 1,783 (C=O), 1,711 (C=O) cm^{-1}; ^{1}H NMR

(200 MHz, DMSO-d_6): $\delta = 7.95$ (s, 1H, Ar), 7.75-7.72 (m, 2H, Ar), 7.42–7.30 (m, 11H, Ar + Ph), 3.79 (s, 2H, H–C(4)) ppm; ^{13}C NMR (50 MHz, DMSO-d_6): $\delta = 177.3$ (C(5)), 173.8 (C(2)), 141.8, 133.2, 132.7, 132.4, 131.0, 130.8, 129.0, 127.8, 118.1, 112.3, 57.1 (C(3)), 44.5 (C(4)) ppm.

Method of calculation

All the calculations were performed using the Gaussian 09 program package [25]. The geometry of the investigated succinimides was fully optimized with DFT B3LYP/6-311G(d,p) and CAM-B3LYP/6-311G(d,p) methods without any constraint on the geometry (for the sake of comparison, the model compound *N*-phenylsuccinimde was recalculated using the MP2 Hamiltonian). The frontier molecular orbital energies and HOMO–LUMO energy gaps were also calculated with the same methods. The natural bond orbital (NBO) analysis [26] was performed using NBO 3.1 program implemented in the Gaussian 09 program package at the same level of theory (results obtained from the B3LYP/6-311G(d,p) calculation are given in the Electronic Supplementary Material). The UV absorption energies of compounds **1a**, **1c**, **1f**, **2a**, **2c**, and **2i** were calculated by the time-dependant DFT method in ethanol solvent on the geometry optimized with the CAM-B3LYP/6-311G(d,p) method in combination with the conductor-like polarizable continuum model (CPCM) [27]. Initially, 50 electron transitions were calculated, but for the purpose of discussion we only considered (unscaled) electron transitions associated with wavelengths longer than 170 nm. The convolution of calculated spectra was done using GaussView 5 [28]. Comparing experimental and calculated spectra, we derived the regression equation ($R^2 = 0.993$), which gives a scaling factor 0.847 and shift 51 nm (results for CAM-B3LYP/6-311G(d,p) and B3LYP/6-311G(d,p) calculations are given in the Electronic Supplementary Material).

To investigate the reactive sites of the succinimides the molecular electrostatic potentials were evaluated using the B3LYP/6-311G(d,p) method and MEP surfaces were plotted for the isosurfaces of 0.002 a.u. electron density.

Acknowledgments This work was performed within the framework of the research Projects Nos. ON 172013 and 172035, supported by the Ministry of Education, Science and Technological Development of the Republic of Serbia.

References

1. LeDuc B (2008) In: Lemke TL, Williams DA (eds) Foye's principles of medicinal chemistry, 6th edn. Lippincott Williams and Wilkins, Philadelphia
2. Coulter DA, Huguenard JR, Prince DA (1989) Ann Neurol 25:582
3. Gomora JC, Daud AN, Weiergräber M, Perez-Reyes E (2001) Mol Pharmacol 60:1121
4. McEvoy GK (ed) (1995) AHFS Drug Information. American Society of Health-System Pharmacists, Bethesda
5. Kamiński K, Obniska J (2008) Bioorg Med Chem 16:4921
6. Obniska J, Byrtus H, Kamiński K, Pawłowski M, Szczesio M, Karolak-Wojciechowska J (2010) Bioorg Med Chem 18:6134
7. Kamiński K, Rzepka S, Obniska J (2011) Bioorg Med Chem Lett 21:5800
8. Murray JS, Abu-Awwad F, Politzer P, Wilson LC, Troupin AS, Wall RE (1998) Int J Quant Chem 70:1137
9. Kwiatkowski W, Karolak-Wojciechowska J (1993) SAR QSAR Environ Res 1:233
10. Obniska J, Zajec A, Karolak-Wojciechowska J (1999) Farmaco 54:423
11. Lapszewicz J, Lange J, Rump S, Walczyna K (1978) Eur J Med Chem 13:465
12. Hansch C, Björkrotahn JP, Leo A (1987) J Pharm Sci 76:663
13. Hadjipavlou-Litina D (1998) Med Res Rev 18:91
14. Abraham MH, Lieb WR, Franks NP (1991) J Pharm Sci 80:719
15. Abraham MH (1993) Pure Appl Chem 65:2503
16. Perisic-Janjic N, Kaliszan R, Wiczling P, Milosevic N, Uscumlic G, Banjac N (2011) Mol Pharm 8:555
17. Kamlet MJ, Abboud JLM, Abraham MH, Taft RW (1983) J Org Chem 48:2877
18. Hofmann K, Brumm S, Mende C, Nagel K, Seifert A, Roth I, Schaarschmidt D, Langc H, Spange S (2012) New J Chem 36:1655
19. Riedel F, Spange S (2012) J Phys Org Chem 25:1261
20. Yu M, Huang X, Gao F (2012) Acta Cryst E 68:o2738
21. Sanna A (1927) Gazz Chim Ital 57:761
22. Barman G, Roy M, Ray JK (2008) Tetrahedron Lett 49:1405
23. Katritzky AR, Nair SK, Witek RM, Hutchins SM (2003) ARKIVOC 5:9
24. Miller CA, Long LM (1951) J Am Chem Soc 73:4895
25. Frisch MJ, Trucks GW, Schlegel HB, Scuseria GE, Robb MA, Cheeseman JR, Scalmani G, Barone V, Mennucci B, Petersson GA, Nakatsuji H, Caricato M, Li X, Hratchian HP, Izmaylov AF, Bloino J, Zheng G, Sonnenberg JL, Hada M, Ehara M, Toyota K, Fukuda R, Hasegawa J, Ishida M, Nakajima T, Honda Y, Kitao O, Nakai H, Vreven T, Montgomery JA, Peralta JE Jr, Ogliaro F, Bearpark M, Heyd JJ, Brothers E, Kudin KN, Staroverov VN, Keith T, Kobayashi R, Normand J, Raghavachari K, Rendell A, Burant JC, Iyengar SS, Tomasi J, Cossi M, Rega N, Millam JM, Klene M, Knox JE, Cross JB, Bakken V, Adamo C, Jaramillo J, Gomperts R, Stratmann RE, Yazyev O, Austin AJ, Cammi R, Pomelli C, Ochterski JW, Martin RL, Morokuma K, Zakrzewski VG, Voth GA, Salvador P, Dannenberg JJ, Dapprich S, Daniels AD, Farkas O, Foresman JB, Ortiz JV, Cioslowski J, Fox DJ (2010) Gaussian 09, revision C.01. Gaussian, Wallingford, CT
26. Glendening ED, Reed AE, Carpenter JE, Weinhold F (1998) NBO version 3.1, TCI, University of Wisconsin, Madison
27. Cossi M, Rega N, Scalmani G, Barone V (2003) J Comput Chem 24:669
28. Dennington R, Keith T, Millam J (2009) GaussView, version 5.0.9. Semichem, Shawnee Mission, KS